Nonequilibrium Phenomena in the Phase Separation of a Two-Component Lipid Bilayer

Rodrigo F. M. de Almeida,* Luís M. S. Loura,*† Aleksandre Fedorov,* and Manuel Prieto*
*Centro de Química-Física Molecular, Instituto Superior Técnico, P-1049-001 Lisboa, Portugal; and †Departamento de Química, Universidade de Évora, Rua Romão Ramalho, 59, P-7000-671 Évora, Portugal

ABSTRACT Lipid bilayers composed of two phospholipids with significant acyl-chain mismatch behave as nonideal mixtures. Although many of these systems are well characterized from the equilibrium point of view, studies concerning their nonequilibrium dynamics are still rare. The kinetics of lipid demixing (phase separation) was studied in model membranes (large unilamellar vesicles of 1:1 dilauroylphosphatidylcholine (C_{12} acyl chain) and distearoylphosphatidylcholine (C_{18} acyl chain)). For this purpose, photophysical techniques (fluorescence intensity, anisotropy, and fluorescence resonance energy transfer) were applied using suitable probes (gel phase probe *trans*-parinaric acid and fluid phase probe *N*-(7-nitrobenz-2-oxa-1,3-diazol-4-yl)-dilauroylphosphatidylethanolamine). The nonequilibrium situation was induced by a sudden thermal quench from a one-fluid phase equilibrium situation (higher temperature) to the gel/fluid coexistence range (lower temperature). We verified that the attainment of equilibrium is a very slow process (occurs in a time scale of hours), leading to large domains at infinite time. The nonequilibrium structure stabilization is due essentially to temporarily rigidified C_{12} chains in the interface between gel/fluid domains, which decrease the interfacial tension by acting as surfactants. The relaxation process becomes faster with the increase of the temperature drop. In addition, heterogeneity is already present in the supposed homogeneous fluid mixture at the higher temperature.

INTRODUCTION

The fluid mosaic model of biological membranes (Singer and Nicolson, 1972) emphasizes membrane fluidity and free lateral diffusion of membrane components. This led to the generalized idea of biomembranes as solutions of proteins embedded in bilayers of randomly distributed phospholipids. However, over the past few years, evidence has accumulated suggesting that the lipid distribution on the bilayer is nonrandom, both in model systems and in biological membranes (Edidin, 1998). In fact, it can exhibit ordered structures with length scales ranging from micrometers (visualized by microscopy; Korlach et al., 1999) to nanometers (mostly indirect evidence, for review, see Mouritsen and Jørgensen, 1997). Particular attention has been dedicated to the gel/fluid coexistence region of binary systems composed of two saturated 1,2-di-acyl-phosphatidylcholines (PC) that differ only with respect to their acyl chain length (creating a hydrophobic mismatch; Mouritsen and Bloom, 1984). In these systems the formation of compositionally distinct domains implies the creation of regions of different bilayer hydrophobic thickness (with a mismatch at the domain interface that has somehow to be compensated; see Introduction section in Schram et al., 1996). Concomitantly, some atomic force microscopy studies have been performed (Mouritsen, 1998; Gliss et al., 1998) with detection of domains on the nanometer range.

Submitted November 1, 2000 and accepted for publication November 13, 2001.

Address reprint requests to Manuel Prieto, Centro de Química-Física Molecular, Instituto Superior Técnico, P-1049-001 Lisboa, Portugal. Tel.: 351-218419219; Fax: 351-218464455; E-mail: prieto@alfa.ist.utl.pt.

0006-3495/02/02/823/12 $2.00

The phase diagram of binary lipid bilayers (like the one in Fig. 1) gives the composition and proportion of each phase in the two-phase (usually gel and fluid) coexistence region but gives no information on the degree of dispersion of one phase in the other. In fact, there is a number of works reporting the existence of small domains and percolative structures in the two-phase coexistence region (Sankaram et al., 1992; Almeida et al., 1992; Piknová et al., 1996; Gliss et al., 1998). This indicates that the phase diagrams like the one in Fig. 1, despite being an important framework, give an incomplete view of the system. Factors that can affect the dispersion of the phases are, e.g., interfacial tension and the curvature of the bilayer (Sackmann and Feder, 1995; Brumm et al., 1996).

In most of the supra cited studies equilibrium conditions are assumed, whereas active and functional membranes are far from equilibrium, or in a steady-state controlled by fluxes of energy and matter. Thus, thermodynamic nonequilibrium effects should have relevance for the lateral organization of membrane components. This issue has been addressed by Mouritsen, Jørgensen, and coworkers in the past few years. Using a microscopic interaction model, they performed Monte-Carlo simulations of the nonequilibrium ordering process of binary lipid mixtures composed of two PC with different acyl chain lengths. Before zero time, the system was equilibrated at a temperature above the liquidus boundary ($T > T_l$), and at zero time it was submitted to an instantaneous thermal quench into the gel/fluid coexistence region, between the solidus and liquidus lines ($T_l > T > T_s$). After this quench, the formation of small lipid domains occurred. These domains grew slowly, originating highly heterogeneous percolative-like structures with a network of interface regions with properties distinct from those of the

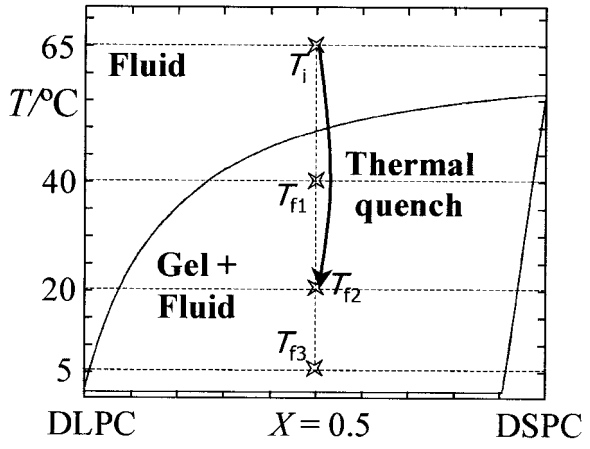

FIGURE 1 Phase diagram for $DC_{12}PC/DC_{18}PC$ vesicles (adapted from Mabrey and Sturtevant, 1976). The initial temperature (T_i) and the three final temperatures (T_f) after the thermal quenches are shown.

separated gel and fluid bulk phases (Mouritsen and Jørgensen, 1994; Jørgensen and Mouritsen, 1995). From the experimental point of view, detailed studies are still scarce. In a very recent study, Fourier-transform infrared spectroscopy and fluorescence intensity measurements indicated the occurrence of slow ordering processes in binary lipid vesicles (Jørgensen et al., 2000).

In the present work, large unilamellar vesicles (LUV) composed of equimolar mixtures of 1,2-dilauroylphosphatidylcholine ($DC_{12}PC$)/1,2-distearoylphosphatidylcholine ($DC_{18}PC$) are used. This system is well characterized from the equilibrium point of view (Mabrey and Sturtevant, 1976; Jørgensen and Mouritsen, 1995). The LUV are first equilibrated at $T > T_l$ and then submitted to a very rapid thermal quench to one of three gel/fluid coexistence temperatures (T_{f1}, T_{f2}, and T_{f3} in Fig. 1), where the system is in a new situation far from equilibrium. The relaxation process is monitored by different photophysical techniques. In the first part of this study, steady-state fluorescence and anisotropy of a probe that partitions preferentially to one of the two coexisting phases are used. In the second part of this work, the relaxation process is followed from the efficiency of time-resolved fluorescence resonance energy transfer (FRET) between a gel phase probe (donor) and a fluid phase probe (acceptor). It is intended to obtain information on the preponderance and stability of conformationally ordered and disordered microenvironments (mainly in the first part) and on the dimensions of those microenvironments on the nanometer scale (mainly in the FRET experiment).

MATERIALS AND METHODS

Sample preparation

$DC_{12}PC$ and $DC_{18}PC$ (chloroform solutions) were from Avanti Polar Lipids (Birmingham, AL). Two fluorescent probes were used, *trans*-parinaric acid (*t*-PnA) and *N*-(7-nitrobenz-2-oxa-1,3-diazol-4-yl)-dilauroylphosphatidylethanolamine (NBD-PE), both from Molecular Probes (Eugene, OR). The purity of NBD-PE (custom synthesis from the supplier) was verified by thin layer chromatography, and a retention factor $R_f = 0.54$ consistent with the published value of 0.53 (Arvinte and Hildenbrand, 1984) was measured. All materials were used as received. *t*-PnA was stocked in ethanol solution and NBD-PE was stocked in methanol solution. Concentrations of the stock solutions were determined spectrophotometrically using molar absorption coefficients of ε(*t*-PnA, 299.4 nm) = 89×10^3 M^{-1} cm^{-1} (Sklar et al., 1977a) and ε(NBD-PE, 463 nm) = 21×10^3 M^{-1} cm^{-1} (Haugland, 1996). LUV of $DC_{12}PC/DC_{18}PC$ (~1 mM total phospholipid) were prepared as described elsewhere (Hope et al., 1985). LUV stability was controlled by sample turbidity. The suspension medium was a 50 mM Tris-HCl, 100 mM NaCl, 0.2 mM ethylenodiaminetetraacetic acid buffer (pH 7.4). Adequate volumes of *t*-PnA stock solution were added to the LUV suspensions to obtain the desired probe/phospholipid ratios (see below). The volume of the ethanol solution never exceeded 1% of the lipid dispersion, so that it would not destabilize the bilayer structure (Vierl et al., 1994). Under the experimental conditions, *t*-PnA incorporates quantitatively in the membrane (Sklar et al., 1979). To prevent slow incorporation into vesicles (Arvinte et al., 1986), NBD-PE was cosolubilized with the adequate amounts of the phospholipid solutions before vesicle preparation. The ratio probe/phospholipid was 1:500 in all steady-state experiments and in the decay measurements of *t*-PnA (determination of the gel/fluid partition coefficient, see below). In the time-resolved FRET measurements, the *t*-PnA (donor):phospholipid ratio was 1:1000 and the NBD-PE (acceptor):phospholipid ratio was 1:80. The final lipid concentration was determined by phosphorus analysis (McClare, 1971). The acceptor concentration in membranes was calculated using ε(NBD-PE, 468 nm) = 20×10^3 M^{-1} cm^{-1} (Loura et al., 2000a). The absorption spectra of probes in vesicle suspensions were corrected for light scattering (Castanho et al., 1997).

All solutions and suspensions containing *t*-PnA were deoxygenated by saturation with nitrogen before being used or stocked to minimize photooxidation (Sklar et al., 1977b). In these conditions, no variation in fluorescence anisotropy was apparent for more than 10,000 s (see Results).

Thermal history of the samples

After LUV preparation, the samples were kept at room temperature overnight. They were incubated at 65°C for 5 h prior to the thermal quench. The sample, under permanent stirring, was then moved to a water reservoir at the final temperature, and the temperature decrease in the sample was controlled to ±0.1°C. The quench was 97% complete after 80 s when the final temperature was 5°C and 100% complete in less than 30 s in the other cases. The samples were then rapidly transferred to the cell holder (which was already at the final temperature) and the measurements started immediately afterwards (zero time).

Absorption and fluorescence measurements

Fluorescence steady-state measurements were carried out with an SLM-Aminco 8100 series 2 spectrofluorimeter (double excitation and emission monochromators, MC-400) in a right angle geometry, the light source being a 450-W Xe arc lamp and the reference a Rhodamine B quantum counter solution. Excitation and emission spectra were corrected using the correction file supplied by the manufacturer. Quartz cuvettes (1 cm × 1 cm) were used. For kinetic studies, stirring was maintained inside the cuvette by a Hellma cuv-o-stir 333 magnetic stirrer. Temperature was controlled to ±0.5°C by a thermostatted cuvette holder. In the case of measurements at 5°C, a mild flow of nitrogen was introduced into the

sample compartment to avoid air humidity condensation in the cuvette walls. The steady-state anisotropy, $\langle r \rangle$, was calculated by Jabłoński (1960)

$$\langle r \rangle = (I_{VV} - G \times I_{VH})/(I_{VV} + 2 \times G \times I_{VH}) \quad (1)$$

in which the different intensities I_{ij} are the steady-state vertical and horizontal components of the fluorescence emission with excitation vertical (I_{VV} and I_{VH}, respectively) and horizontal (I_{HV} and I_{HH}, respectively) to the emission axis. The latter pair of components is used to calculate the G factor ($G = I_{HV}/I_{HH}$; Chen and Bowman, 1965). Polarization of excitation and emission light was achieved using Glan-Thompson polarizers. Blank subtraction was taken into account.

Absorption spectroscopy data were obtained with a Shimadzu UV-3101PC spectrophotometer.

The instrumentation for fluorescence decay measurements by the single photon-timing technique with pulsed laser excitation has been described (Loura et al., 1996). Two cut-off filters were added to the system to further screen scattered excitation light and isolate donor fluorescence from that of acceptor. Excitation (at 303 nm) was vertically polarized and emission (at 405 nm) was detected at 54.7° relative to the excitation beam. The number of counts on the peak channel was between 10,000 and 20,000. The number of channels per curve used for analysis was ~1000, with a time scale of 0.332 ns/channel. Data analysis was performed as previously described (Loura et al., 1996). Fluorescence decays were obtained on 5 mm × 5 mm quartz cuvettes. In the FRET measurements, an aliquot (400 μl) was taken from the sample without acceptor (D sample) to a cuvette, and counts were accumulated for 5 min. Subsequently, an aliquot was taken from the sample with acceptor (DA sample) to an identical cuvette, and counts were accumulated also for 5 min. Then the pulse profile was obtained from a scatter dispersion (silica, colloidal water suspension, Aldrich, Milwaukee, WI). This procedure was repeated for several hours. The samples were submitted to a 1-min flow of nitrogen and carefully sealed after removing each aliquot. During the course of the experiments, the decay parameters of the donor in the absence of acceptor were invariant for more than 15,000 s (see Results). The time ascribed to each experimental point was the average between the start of each measurement of a D sample and the end of the measurement of the respective DA sample. Energy transfer efficiency, E, was calculated according to

$$E = 1 - \bar{\tau}_{DA}/\bar{\tau}_{D} \quad (2)$$

in which $\bar{\tau}_{D}$ and $\bar{\tau}_{DA}$ are the lifetime-weighted quantum yields of the donor in the absence and in the presence of acceptor, respectively. The lifetime-weighted quantum yield is in turn defined by (Lakowicz, 1999)

$$\bar{\tau} = \sum_{i} \alpha_i \tau_i \quad (3)$$

for a decay described by a sum of exponentials, in which α_i are the normalized preexponentials and τ_i the lifetime of the decay component i. Average fluorescence lifetimes were calculated by (Lakowicz, 1999):

$$\langle \tau \rangle = \sum_{i} \alpha_i \tau_i^2 \Big/ \sum_{i} \alpha_i \tau_i \quad (4)$$

RESULTS

Probe photophysics

Fig. 2 shows the absorption and emission spectra of the donor (*t*-PnA) and the acceptor (NBD-PE) incorporated in $DC_{12}PC/DC_{18}PC$ (1:1) LUV at 20°C, showing the large overlap of donor emission and acceptor absorption.

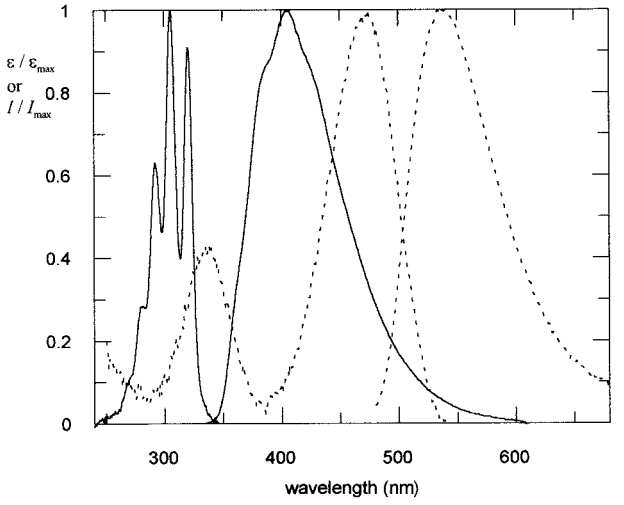

FIGURE 2 *t*-PnA (*solid lines*) and NBD-PE (*dashed lines*) absorption and corrected fluorescence (excitation at 306 and 468 nm, respectively) normalized spectra in equimolar $DC_{12}PC/DC_{18}PC$ LUV at 20°C.

NBD-PE in LUV of $DC_{12}PC/DC_{18}PC$ (1:1) displays absorption and emission maxima at 466 and 536 nm, respectively, which are close to reported maxima in methanol solution (Haugland, 1996) and in membranes (Chattopadhyay and London, 1988). The fact that the maximum of the measured emission spectrum lies at 536 nm shows that the chromophore is in a rather polar environment (Chattopadhyay, 1990). In fact, this wavelength corresponds to the maximum of emission intensity when the probe is in a solution of water/ethanol 1:3 (Arvinte et al., 1986). This is in agreement with the expected position of the NBD moiety, which is in the water/phospholipid polar head group interface.

t-PnA has an emission maximum at 406 nm independent of the LUV composition. With respect to the absorption, maxima occur at 320, 305.5, 292, and 281.5 nm (shoulder) for equimolar $DC_{12}PC/DC_{18}PC$ LUV, which are practically coincident with those for chloroform solution (Sklar et al., 1977a). However, with varying composition, a 3-nm red shift occurs (peak at ~320 nm, $0 \leftarrow 0$ transition), which depends on the gel phase fraction, X_g (results not shown). Sklar et al. (1977a,b) proposed and validated a simple method for the calculation of the relative density change correspondent to a given spectral shift and the effective refractive index, n, in lipid bilayers using the wavelength of the $0 \leftarrow 0$ vibronic transition. This method is based on the fact that the energy of the transition of a linear polyene (apolar chromophore) in an apolar solvent is linearly related to the solvent polarity function $f(n^2) = (n^2 - 1)/(n^2 + 2)$ (Suppan and Ghoneim, 1997), which is in the present conditions proportional to the density of the medium (Sklar et al., 1977b). Applying this method for LUV of $DC_{12}PC/DC_{18}PC$ at 20°C, we obtain $n = 1.50$ for the gel and $n = 1.44$ for the fluid.

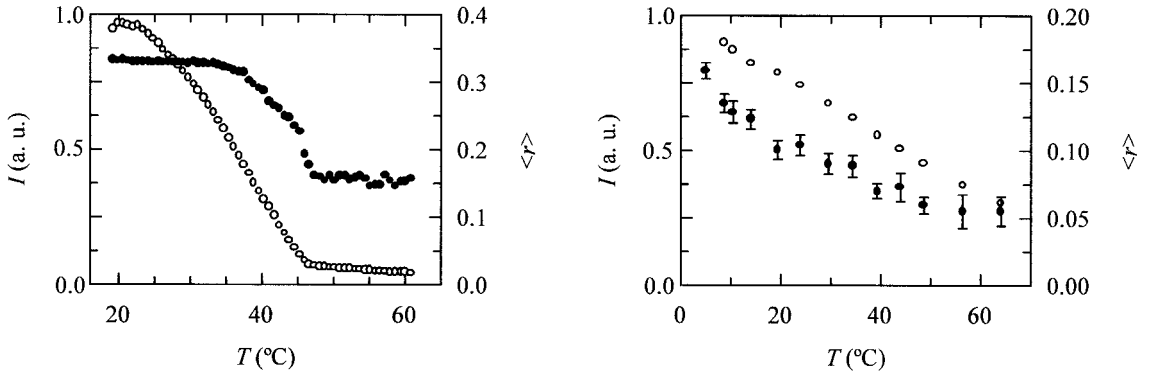

FIGURE 3 Steady-state fluorescence (○) and anisotropy (●) of *t*-PnA (*left panel*) and NBD-PE (*right panel*) in equimolar $DC_{12}PC/DC_{18}PC$ LUV equilibrated at different temperatures. Error bars (standard error of the mean) are shown where thicker than data points.

These values are very close to the values of $n = 1.49$ and 1.46 for 1,2-dipalmitoylphosphatidylcholine ($DC_{16}PC$) right below and above the gel to liquid crystalline transition temperature, respectively (Sklar et al., 1977b). The correspondent gel:fluid density ratio is $\rho_g/\rho_f = 1.12$. Calculating ρ_g/ρ_f from a partial specific volume of 0.963 ml/g for $DC_{12}PC$ at 20°C and 0.943 ml/g for DSPC at 21°C (Marsh, 1990), and considering $X_{DC18PC}^{gel} \sim 1$ and $X_{DC12PC}^{fluid} \sim 1$, a value of 1.02 is obtained (*X* stands for mole fraction). However, if the ratio ρ_g/ρ_f is calculated from the molecular volumes of constituent molecular groups (Marsh, 1990), taking the gel as pairs of C_{18} acyl chains in the gel state and the fluid as pairs of C_{12} acyl chains in the fluid state, the value $\rho_g/\rho_f = 1.11$ is recovered, in close agreement with the value obtained from the *t*-PnA absorption shift. This confirms that the environment of the tetraene chromophore of *t*-PnA is the acyl chain apolar region of the bilayer (Castanho et al., 1996).

Fig. 3 shows the fluorescence intensity (*I*) and anisotropy ($\langle r \rangle$) of *t*-PnA (*left panel*) and NBD-PE (*right panel*) in equilibrated LUV of $DC_{12}PC/DC_{18}PC$ 1:1 as a function of temperature. Regarding *t*-PnA, the curves reflect the preference of this probe for the gel phase. This is more apparent for the $\langle r \rangle$ variation, because for this probe this parameter is less sensitive to temperature than *I* and also because it is proportional not to the amounts of probe in each phase (as occurs for *I*) but to their respective emission. This behavior has been observed previously for *t*-PnA incorporated in $DC_{16}PC$ vesicles (Sklar et al., 1977b) and phospholipid mixtures (Sklar et al., 1979). In the case of NBD-PE, both *I* and $\langle r \rangle$ show a systematic decrease of their values with increasing temperature. In the case of *I*, the decrease occurs with an approximately constant slope, whereas in the case of $\langle r \rangle$ some stabilization after complete disappearing of the gel phase is apparent. The relative decrease of *I* between 22°C and 40°C is in very good agreement with the respective decrease of the lifetime-weighted quantum yield $\bar{\tau}$ (Loura et al., 2000b).

From the photophysical parameters Förster radius were determined according to (e.g., Berberan-Santos and Prieto, 1987),

$$R_0 = 0.02108 \times \left[\frac{(\int \lambda^4 \varepsilon_A(\lambda) f_D(\lambda) d\lambda) \kappa^2 \Phi_D}{n^4} \right]^{1/6} \quad (5)$$

R_0(gel phase) = 37.2 Å and R_0(fluid phase) = 24.4 Å being obtained. In Eq. 5, $f_D(\lambda)$ is the normalized fluorescence of the donor, ε_A is the acceptor molar absorption coefficient, κ^2 is the orientation factor, and Φ_D is the donor quantum yield. The numerical constant is valid for units of nm for λ, $M^{-1}\,cm^{-1}$ for ε and Å for R_0. A value of 2/3 was used for κ^2 (dynamic isotropic limit) and 1.4 for *n* (average between the refractive index of water and the values obtained for the lipid phases).

The fluorescence properties of *t*-PnA have been intensely studied both in isotropic solvents and in lipid bilayers. The fluorescence decays of the probe are well described by the sum of two exponentials (or by bimodal functions in continuous distribution analysis) in isotropic solvents and in bilayers in the fluid state (Ruggiero and Hudson, 1989; Mateo et al., 1993). Biexponential decays were reported also for the gel phase (Wolber and Hudson, 1981). In that work, the lifetimes of the two components in LUV of $DC_{18}PC$ at 23°C for a phosphatidylcholine with a *t*-PnA tail substitution were 12.7 and 61.0 ns, in excellent agreement with our results for the gel phase (Table 1). In the samples with varying composition, the long component lifetime remained constant and its amplitude increased with the gel phase fraction X_g. For these reasons and on account of other authors' works (Ruggiero and Hudson, 1989; Mateo et al., 1993), the long component can unequivocally be attributed to probe located in the gel phase. At our best knowledge, the measured value is the longest reported for *t*-PnA in bilayers. It seems therefore that the gel phase in $DC_{12}PC/DC_{18}PC$ bilayers at 20°C is remarkably rigid.

The decays for *t*-PnA are described essentially by two short components when only fluid phase is present (lipid

TABLE 1 Time-resolved fluorescence decay parameters of *t*-PnA in $DC_{12}PC/DC_{18}PC$ LUV (20°C) for different gel phase fractions (X_g)

X_g	α_1	τ_1 (ns)	α_2	τ_2 (ns)	α_3	τ_3 (ns)	$\bar{\tau}$ (ns)	$\langle\tau\rangle$ (ns)	χ^2
0	0.57	2.1	0.43	6.0	<0.01	62.9	4.7	9.9	1.27
0.21	0.43	3.6	0.15	17.3	0.42	66.6	32.0	59.5	1.14
0.51	0.16	4.1	0.16	21.7	0.68	65.9	48.9	61.8	1.25
0.82	0.11	11.2	0.16	30.5	0.73	66.4	54.4	61.9	1.12
1	0.21	23.3	–	–	0.79	65.5	56.4	61.7	1.18

α_i are the normalized preexponentials and τ_i the lifetime of the decay component i. $\bar{\tau}$ is the lifetime-weighted quantum yield (Eq. 3) and $\langle\tau\rangle$ is the average lifetime (Eq. 4).

molar fraction of gel, $X_g = 0$), one intermediate and one long component when $X_g = 1$, and three components for intermediate X_g values (Table 1). The one-phase samples were prepared with the same overall composition as the respective phase in the other samples, according to the phase diagram. Consequently, the long component observed on the fluid phase sample, with a very small contribution to the total decay, can be due to uncertainties on the $DC_{12}PC$:$DC_{18}PC$ ratio. An additional possibility is the occurrence of density fluctuations because the coexistence region is contiguous to the liquidus line (Ruggiero and Hudson, 1989). Within the gel/fluid coexistence region, the need to use three exponentials has been reported (Mateo et al., 1993). As expected, the lifetime-weighted quantum yield (Eq. 3) increased with increasing gel phase fraction and this effect was used to determine the partition coefficient between the gel and the fluid lipid phases for *t*-PnA. The gel/fluid partition coefficient is defined by

$$K_p^{g/f} = \frac{n_g/X_g}{n_f/(1 - X_g)} \tag{6}$$

in which n_g and n_f are the amounts of probe in the gel and fluid phase, respectively. $K_p^{g/f}$ can be obtained from the $\bar{\tau}$ of *t*-PnA as a function of X_g through the following expression (Loura et al., 2000b):

$$\bar{\tau} = \frac{\bar{\tau}_g K_p^{g/f} X_g + (1 - X_g)\bar{\tau}_f}{K_p^{g/f} X_g + (1 - X_g)} \tag{7}$$

in which $\bar{\tau}_f$ and $\bar{\tau}_g$ are the lifetime-weighted quantum yields of probe in the fluid and in the gel, obtained for the samples with $X_g = 0$ and $X_g = 1$, respectively. From this single parameter fit, a $K_p^{g/f}$ of 4.8 ± 0.5 was recovered (Fig. 4). This is in agreement with values found on the literature (Sklar et al., 1979), and being significantly higher than unity, the preference of the probe for the ordered phase is verified.

Steady-state fluorescence and anisotropy

Fig. 5 shows the time evolution of steady-state fluorescence intensity, I (*left plots*), and anisotropy, $\langle r\rangle$ (*right plots*), of

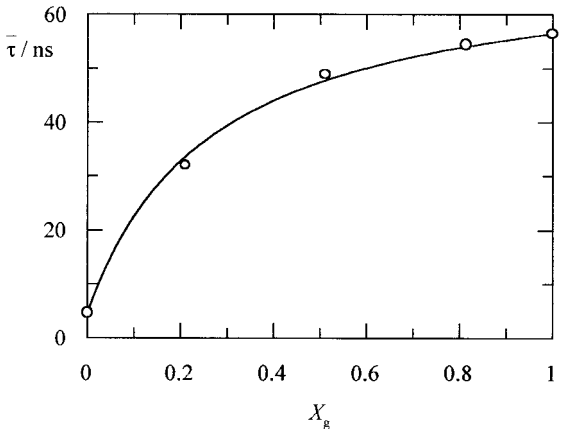

FIGURE 4 *t*-PnA lifetime-weighted quantum yield versus composition of $DC_{12}PC/DC_{18}PC$ LUV at 20°C. Best fit of Eq. 7 ($K_p^{g/f} = 4.8 \pm 0.5$) is shown.

NBD-PE after a thermal quench at zero time from 65°C to 5, 20, and 40°C. In every case, there is a fast increase in both I and $\langle r\rangle$, surpassing the equilibrium value ("overshoot"), followed by a slow decay. These decays are well described by a single exponential function with nonzero limit (an offset that corresponds to the equilibrium parameter), yielding relaxation times of the order of hours (see insert in each plot). This behavior is at variance with *t*-PnA, for which constant $\langle\tau\rangle$, $\bar{\tau}$, and $\langle r\rangle$ values consistent with the values measured in equilibrated samples (Figs. 3 and 4) were measured immediately after zero time (Fig. 6). Reproducibility of the results was verified for both probes. We should stress that the exponential function merely intends to describe empirically the time-evolution of the system (probably, this process resembles spinodal decomposition (Jørgensen and Mouritsen, 1995), for which a theoretical rationalization of the fluorescence data would be complex).

Additionally, for NBD-PE, an inverse relation of relaxation rates with temperature is observed, i.e., the decay is faster when the temperature change is larger. The overshoot duration (delay time) is not so reproducible, and this is possibly due to variations in the rapidity of the quench. In any case, the general trend is the same as that observed for the relaxation times. The asymptotic values of $\langle r\rangle$ increase with decreasing temperature, as expected on the basis of slower rotational diffusion (Weber, 1953), and their values are in accordance with the equilibrium ones (Fig. 3).

Kinetics of FRET efficiency from time-resolved fluorescence

The decays of *t*-PnA in the presence of NBD-PE are additionally complex due to intermolecular FRET (Fung and Stryer, 1978). Three exponential fits to these decays were performed with the sole purpose of integrating the curve to obtain $\bar{\tau}_{DA}$, no physical meaning being attributed to the

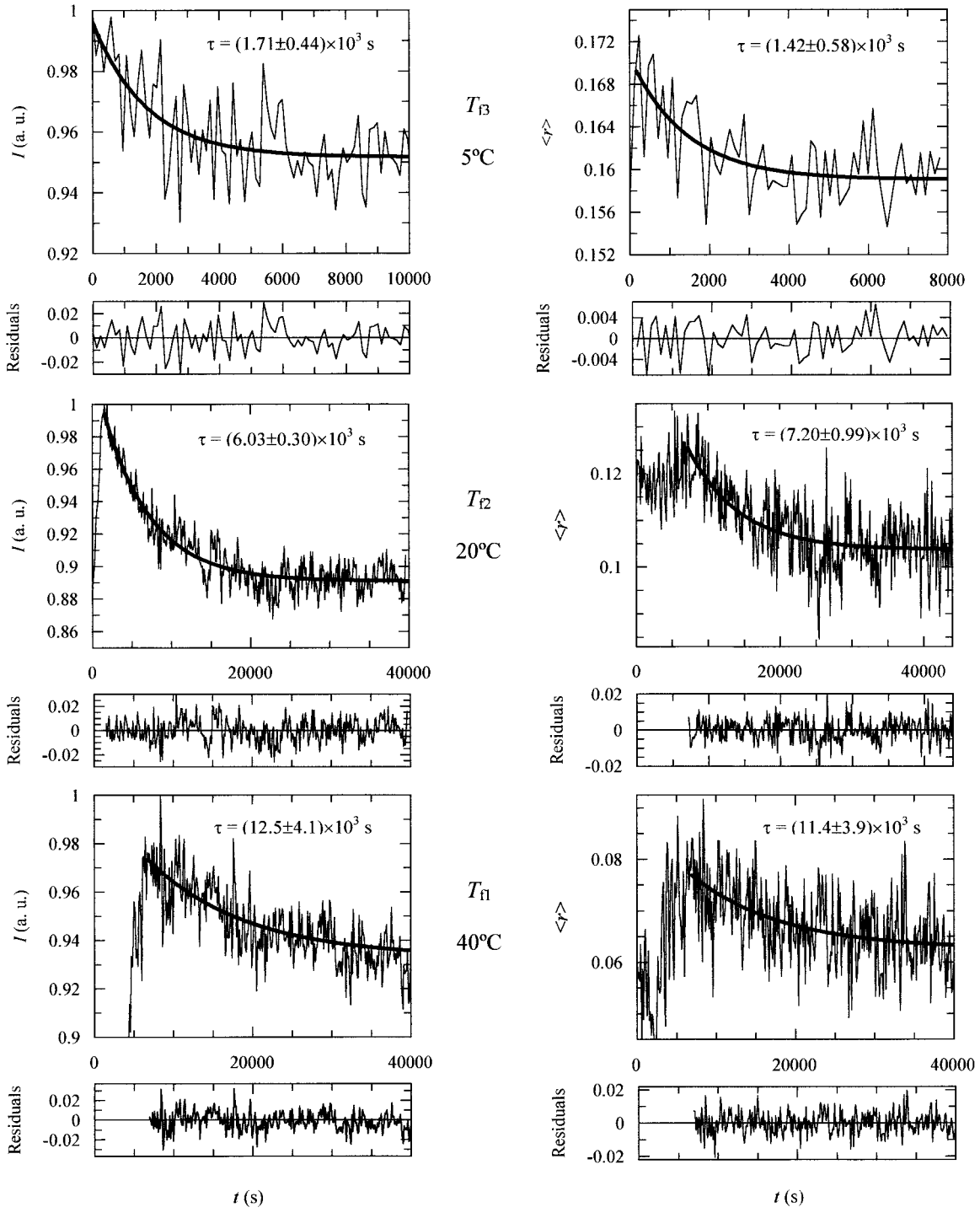

FIGURE 5 Steady-state fluorescence (*left*) and anisotropy (*right*) of NBD-PE in equimolar $DC_{12}PC/DC_{18}PC$ LUV versus time. The sample was initially equilibrated at $T = 65°C$ on the fluid phase region. Then it was suddenly quenched to a final temperature of 5, 20, or 40°C in the gel/fluid coexistence region. The thick line is the fit of a single exponential function with relaxation time τ (indicated for each plot together with respective standard error) and a nonzero limit value to the decay part of the experimental data points. The residuals of the fit are also shown.

components. The choice of three exponentials is justified by the fact that they describe the decays adequately in statistical terms (in all cases reduced $\chi^2 \leq 1.3$), and no significant improvement was obtained by increasing the number of components. The FRET efficiency, E, was then calculated through Eq. 2, and the results plotted in Fig. 7. It can be seen

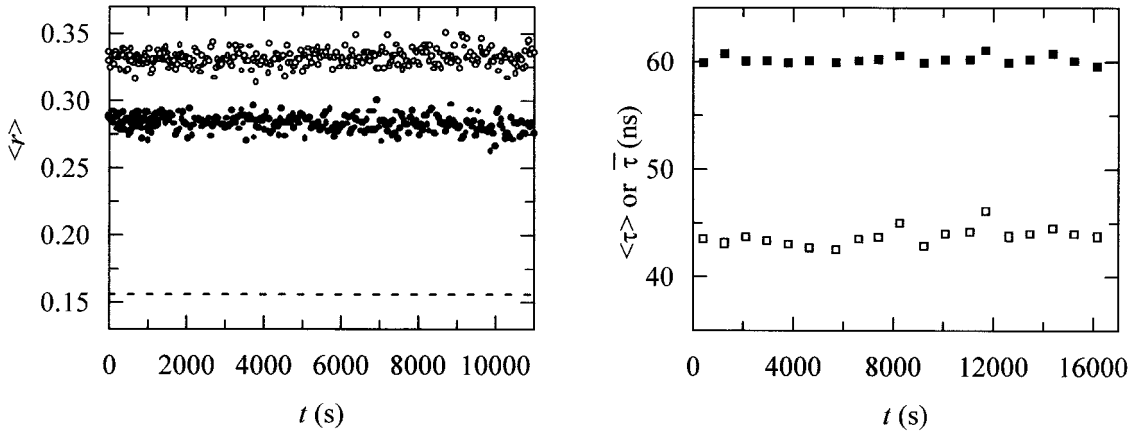

FIGURE 6 Time-evolution of the fluorescence properties of *t*-PnA in equimolar $DC_{12}PC/DC_{18}PC$ LUV after a sudden thermal quench at zero time from $T = 65°C$ in the fluid phase region to a temperature T_f in the gel/fluid coexistence region. (*Left panel*) Steady-state anisotropy ($T_f = 5$ or 20°C (○) and $T_f = 40°C$ (●)); the value for the fluid phase is also shown for comparison (- - -). (*Right panel*) Fluorescence lifetime $\langle\tau\rangle$ (Eq. 4, ■) and lifetime averaged quantum yield (Eq. 3, □) are shown; $T_f = 20°C$ in both cases.

that E decreases with time, and an exponential function with an offset $E = E(t = 0)\exp(-t/\theta) + E(t = \infty)$ is a reasonable empirical description of the results (θ is the relaxation time). The best fit parameters are: $E(t = 0) = (26.8 \pm 1.7)\%$, $E(t = \infty) = (19.0 \pm 0.9)\%$, and $\theta = (6.9 \pm 2.1) \times 10^3$ s.

DISCUSSION

Steady-state fluorescence and anisotropy

Experimental kinetic studies of lipid demixing in membranes are very scarce in the literature, but a detailed theoretical framework using Monte-Carlo simulations was developed recently (Mouritsen and Jørgensen, 1994; Jørgensen and Mouritsen, 1995; Jørgensen et al., 2000).

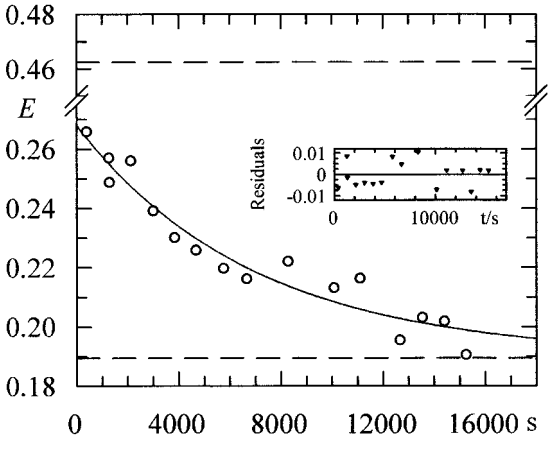

FIGURE 7 Energy transfer efficiency (calculated from transient-state fluorescence measurements, Eqs. 2 and 3) from *t*-PnA to NBD-PE versus time. Experimental conditions: equimolar $DC_{12}PC/DC_{18}PC$ LUV after a sudden thermal quench from $T = 65°C$ (fluid phase region) to a final temperature $T_{f2} = 20°C$ in the gel/fluid coexistence region. The line is the best fit of an exponential function with a nonzero limit value, and the residuals are shown in the insert. The two limiting E values were calculated assuming totally random distribution of both probes at zero time (Eqs. 9–11; *dashed line* above in the plot) and complete phase separation at infinite time (Eqs. 10–12; *dashed line* below in the plot).

The time-dependence observed for I and $\langle r\rangle$ of NBD-PE (slow decay; Fig. 5) and the time invariance for *t*-PnA (Fig. 6) was parallel to that obtained for the average chain order parameter of $DC_{12}PC$ and $DC_{18}PC$, respectively, in the Monte-Carlo simulation of an equimolar mixture of $DC_{12}PC/DC_{18}PC$ after a thermal quench from $T = 57°C > T_l$ to $T = 5°C$ between T_s and T_l (Mouritsen and Jørgensen, 1994). *t*-PnA partitions preferentially to the gel phase and has higher quantum yield and anisotropy in that phase than in the fluid. While at the higher temperature the probe is within the fluid because this is the only phase present, at the two-phase coexistence temperature the fluorescence parameters of *t*-PnA probe reflect essentially the behavior of the gel state lipids. NBD-PE partitions preferentially to the fluid ($K_p^{g/f} = 0.16$ at 20°C, Loura et al., 2000b). The anisotropy is significantly larger in the gel, but the quantum yield is only ~5 to 20% higher, as determined from fluorescence decay measurements in membranes with different X_g values (Loura et al., 2000b). Thus, the signal coming from NBD-PE in equilibrium has a main contribution from the fluid. Since before zero time there is only fluid phase, the overshoot of the equilibrium value can only be explained as coming from NBD-PE entrapped in quickly frozen gel domains and that did not have the time to diffuse to $DC_{12}PC$ enriched fluid regions or from NBD-PE molecules with gel-conformation acyl chains in the interfaces surrounding gel domains. This would correspond to a wetting layer of gel-like $DC_{12}PC$ (and analog fluorescent molecules), which chain length lies between the hydrophobic thickness of the gel and fluid phases. The molecules in this layer act as surfactants, decreasing the interfacial tension (driving force for phase separation; Jeppesen and Mouritsen, 1993) and

thus providing a transient stabilization of the nonequilibrium structure (Mouritsen and Jørgensen, 1994; Jørgensen and Mouritsen, 1995). It should be stressed that the relaxation times in Fig. 5 are on the time scale of hours. This behavior reflects primarily what happens to $DC_{12}PC$ (major component of the fluid, Fig. 1). The fluorescence behavior of *t*-PnA reveals that the newly formed gel is probably very similar to the gel in equilibrated samples. The behavior of NBD-PE shows that what is going to be a fluid phase in equilibrium has to evolve from a very different nonequilibrium structure. The overshoot phenomenon in fluorescence intensity and anisotropy reflects that initially there is a large fraction of the short-chain lipid molecules in a conformationally ordered state, which is decreasing with time. In one cited Monte-Carlo study (Jørgensen and Mouritsen, 1995) it was suggested that the fraction of $DC_{12}PC$ in a condensed state and in the boundary region between gel and fluid domains should be very large and decrease with time, approaching the equilibrium value of X_{DC12PC}^{gel} (because the interfacial fractional area becomes close to zero at very long times). The snapshots of the microconfigurations in the mentioned simulations (Mouritsen and Jørgensen, 1994; Jørgensen and Mouritsen, 1995) also indicate that the condensed $DC_{12}PC$ molecules fill to a large extent a region that at later times develops into fluid.

Recently, Jørgensen et al. (2000) studied experimentally phase separation dynamics in equimolar mixtures of $DC_{16}PC$/1,2-dibehenoylphosphatidylcholine ($DC_{22}PC$). This is another example of a system with a broad gel/fluid coexistence range. These authors observed a decrease of the fluorescence intensity of an acyl-chain pyrene-labeled PC after a thermal quench occurring in a timescale of ~2000 to 3000 s, similar to those represented in Fig. 5 for NBD-PE in $DC_{12}PC/DC_{18}PC$.

It could be argued that what is being reported is simply the slow diffusion of NBD-PE from the gel to the fluid phase instead of the evolution of the nonequilibrium domain structure. The argument would be that initially the probe has an approximately homogeneous distribution, against the equilibrium behavior given by a $K_p^{g/f}$ lower than one. However, this is most unlikely, as explained below.

The average time for a collision between two molecules with diffusion coefficient D, randomly distributed in the surface of a sphere of radius r is given by (Tachyia, 1987):

$$\tau_{av} = \frac{r^2}{D}\left[\frac{2}{1-(d/2r)^2}\ln\frac{2r}{d} - 1\right] \qquad (8)$$

in which d is the sum of the molecular radii. Taking $r = 50$ nm (the size of the vesicles used in this work) and $D = 10^{-10}$ cm^2 s^{-1} (typical gel phase diffusion coefficient), one obtains $\tau_{av} \approx 1$ s, a value 10^3 to 10^4 smaller than the measured relaxation times. By the same argument, one must also conclude that diffusion of $DC_{12}PC$ lipids from gel phase structures to disordered phase regions cannot be the only mechanism in the phase separation process. This fact was also recognized by Jørgensen et al. (2000), who claimed that the slowness of the ordering process for $DC_{16}PC/DC_{22}PC$ mixtures might be intimately related to the formation of a wetting layer of ordered low-temperature melting lipids, which would act as two-dimensional surfactants, slowing the interface dynamics and promoting metastability of nonequilibrium domains. In turn, the very presence of this transient but stabilized small gel domains and the extensive interface surrounding them act as further obstacles to lipid diffusion (Almeida et al., 1992). This would be most important in the early stages of phase separation. At later times, closer to equilibrium, the domains are larger, and the interface region is much diminished. In these circumstances, those interfacial effects are less important, and long-range diffusion should be the limiting process for attainment of equilibrium (Jørgensen and Mouritsen, 1995).

Two additional arguments for the complexity of the phase separation mechanism should be emphasized. First, if the sole process were diffusion of lipid from the gel domains to the fluid phase, the relaxation rate would increase with temperature, whereas the opposite is observed. Second, even if initially the probe were in the gel phase, this would not account for the difference between the maximum I value and the equilibrium value. At 20°C, the quantum yield of the probe on the gel is only ~5% higher than in the fluid (Loura et al., 2000b), and the maximum and minimum values in Fig. 5 are ~10% apart. This also shows that the properties of the nonequilibrium phase (consisting of lipid molecules that will evolve to fluid phase) are different from those of both the gel and the fluid in equilibrium.

The quench to different temperatures reveals that the deeper the quench, the faster the phase separation. Because the slow equilibration process concerns especially the fluid phase, we should focus our discussion on it. There is a three- to fourfold increase in the rate of relaxation when the final temperature is changed from 20 to 5°C. Considering that the fluid phase fraction in equilibrium, X_f, is 0.49 at 20°C and 0.47 at 5°C (from Fig. 1), it is unlikely that the difference in X_f accounts for the variation in the kinetics of phase separation. The driving force for the process can be thought of as the distance of the initial condition to equilibrium. This is related to the distance from the point at each temperature corresponding to $X_{DC18PC} = 0.5$ to the point of the liquidus line at the respective temperature. As can be observed in Fig. 1, that distance is larger when the final temperature is lower. The so-called nonequilibrium excess free energy is the driving force for the separation process, and the same relation between the depth of the quench and the rate of the process has been reported for polymer solutions with spinodal decomposition (Tomlins and Higgins, 1989).

It should be noted that the resemblance of the observed relaxation to spinodal decomposition probably stems from the fact that in both of these processes there is a large jump into the biphasic region. If the cooling process was sufficiently slow, and relaxation took place in a quasiequilibrium manner (away

from spinodal decomposition conditions), then the evolution of the system would most probably be different.

Kinetics of FRET efficiency from time-resolved fluorescence

Whereas the acceptor chromophore is located near the water-lipid interface, the donor polyene chromophore is located in the bilayer interior, as discussed above. The transverse distance between the conjugated system of *t*-PnA and the water lipid interface, d, was estimated to be 12.1 Å on the basis of molecular models. In principle, a *t*-PnA molecule located in one bilayer leaflet could transfer its excitation energy to an NBD-PE molecule in either of the two leaflets. However, given the fact that R_0 is less than the bilayer thickness in both phases (see Probe photophysics), for the sake of theoretical estimation of E, we will only consider FRET within the same bilayer leaflet (the contribution of transmembrane FRET to the FRET efficiency is negligible). The time dependence of the donor fluorescence in a situation of intermolecular FRET between donors in one plane and acceptors in a parallel plane at a distance d is given by (Davenport et al., 1985)

$$i_{DA}(t) = i_D(t) \times \exp\left\{-\frac{2c}{\Gamma(2/3)b} \times \int_0^1 [1 - \exp(-tb^3\alpha^6)]\alpha^{-3}d\alpha\right\} \quad (9)$$

in which $i_D(t)$ is the donor decay in the absence of acceptor, $b = (R_0/d)^2/\bar{\tau}^{-1/3}$, and c is proportional to the acceptor concentration, n_A, given by

$$c = \Gamma(2/3)n_A\pi{R_0}^2/\bar{\tau}^{1/3} \quad (10)$$

in which Γ is the complete gamma function. Eq. 9 is valid for homogeneous distribution of probes, and it can be used for calculation of zero-time E (assuming homogeneous distribution in these conditions), after integration:

$$E = 1 - \int_0^\infty i_{DA}(t)dt \Big/ \int_0^\infty i_D(t)dt \quad (11)$$

Using the R_0 values given above and an area/lipid molecule of 54.7 Å^2 for the gel phase (value for pure $DC_{18}PC$ at 25°C; Marsh, 1990) and 68.7 Å^2 for the fluid phase (value for pure $DC_{12}PC$ at 25°C; Marsh, 1990), we calculated $E = 0.46$. This value is considerably larger than the extrapolated experimental value $E(t = 0) = 0.27$ (Fig. 7). The probable origin for this discrepancy is that the probe distribution in the unquenched fluid phase is already nonhomogeneous, confirming the simulation predictions for the $DC_{12}PC$/$DC_{18}PC$ mixture (Mouritsen and Jørgensen, 1994). This does not exclude the additional possibility of a faster regime to occur for initial steps in phase separation, which could not be detected in our experiment. In this case, the extrapolation of E to zero time would represent the value at the onset of the slower process. However, this cannot be confirmed from our data, and is at variance with simulation predictions (Jørgensen and Mouritsen, 1995). On another hand, fluid-fluid heterogeneity has been reported for binary systems in which the main transition temperature differs significantly (e.g., Melchior, 1986).

As shown in Fig. 7, there is a clear decrease of FRET efficiency between *t*-PnA and NBD-PE following a thermal quench to 20°C. This result shows that the donor and acceptor molecules become more apart from each other, as a consequence of the thermal quench. As phase separation occurs, the *t*-PnA molecules in the growing gel phase domains become increasingly more distant from the NBD-PE molecules in the (also growing) fluid domains, hence the reduction in E. Fig. 7 shows that this process occurs in a time scale of hours, and the shape of the E decay curve is, in fact, quite similar to those of I and $\langle r\rangle$ for NBD-PE at the same temperature, apart from the absence of the overshoot at initial times. In this way, it is natural to conclude that both experiments reflect the complementary features of the same phenomenon: the slow growth of the phase separated domains. The E curve, due to the strong dependence of this observable on the donor-acceptor distance, shows in a direct manner the continued increase of domain size with time (hence, no overshoot is apparent in this case). The I and $\langle r\rangle$ curves show the decrease of the fraction of temporarily rigidified interfacial low-melting lipid (as discussed above), a necessary consequence of this domain growth. Thus, it comes as no surprise that the E curve, and the I and $\langle r\rangle$ curves at 20°C, have very similar relaxation times.

Just as important as the zero time limit is the asymptotic regime for $t \to \infty$. The comparison of the experimentally determined value with that predicted assuming complete phase separation can reveal whether in thermodynamic equilibrium there is complete phase separation or small stable domains.

The time-resolved fluorescence of donor in a complete phase separation situation is given by a modification of Eq. 9, allowing for different donor and acceptor populations, corresponding to the gel and fluid phases:

$$i_{DA}(t) = \sum_{j=f,g} i_{Dj}(t)\exp\left\{-\frac{2c_j}{\Gamma(2/3)b_j} \times \int_0^1 [1 - \exp(-tb_j^3\alpha^6)]\alpha^{-3}d\alpha\right\} \quad (12)$$

In this equation, c_j has the same meaning (for phase j, fluid (f) or gel (g)) as c in Eq. 9. These values can be calculated

a priori using the phase diagram information and $K_p^{g/f} = 0.16$ (Loura et al., 2000b) together with the mentioned areas/lipid molecule in each phase. i_{Dj} is the decay of donor in the absence of acceptor, in phase j (Table 1). From these calculations, a value of $E = 0.19$ is recovered, in excellent agreement with the experimental asymptotic value (Fig. 7).

This observation shows that either phase separation is complete, or the persisting domains have sizes larger than those that can be probed using FRET. From Monte-Carlo simulations, this value in intermolecular FRET is ~5 to 10 R_0 (Loura et al., 2001). If there were domains of size $\leq$ 3 to 5 R_0, there could be large probability of FRET between donor on gel domains and acceptor on fluid regions, leading to higher E values (which would, in fact, lie between the limits for random distribution and complete phase separation). Our results show that this is not the case, and this kind of transfer is negligible relative to FRET within the same lipid phase.

It is now worthwhile readdressing the issue of the large variety of domain sizes reported in the literature, ranging from hundreds of molecules (Sankaram et al., 1992) to ~1-μm domains (Coelho et al., 1997). In our opinion, there could be three main sources of discrepancy in this matter: 1) the different techniques used for each case (electron spin resonance spectroscopy, FRAP), which are not sensitive to the same length scales (Dolainsky et al., 1997); 2) the different systems studied (small and large vesicles, multibilayers); and 3) even though the previous points may be the most important, there is an additional factor, often overlooked, which is the slow kinetics of phase separation. Although this has admittedly been suspected of and prevented by researchers who describe long equilibration times, our study describes an experiment that actually provides the timescales of equilibration for some systems. This work shows that this process can take hours for the $DC_{12}PC/DC_{18}PC$ system, similarly to the $DC_{16}PC/DC_{22}PC$ system (Jørgensen et al., 2000). For the 1,2-dimyristoylphosphatidylcholine ($DC_{14}PC$)/$DC_{18}PC$ system (in which most literature studies are carried out), the demixing kinetics following a large temperature quench may be even slower, because the driving force for the process is in this case less significant (greater lipid miscibility/smaller acyl chain mismatch). Therefore, equilibration time for this type of systems can be particularly critical, and awareness of this fact is crucial for the design of future experiments. A larger percentage of the short chain component should also correspond to a slower process, as the initial point will be closer to the liquidus line. Indeed, in a preliminary study, we obtained a relaxation time of $(1.53 \pm 0.38) \times 10^4$ s when a $DC_{12}PC/DC_{18}PC$ (3:1) mixture is cooled from 65 to 20°C, which is twice as large as the value for the 1:1 mixture (Fig. 5). Studies in other lipid mixtures, eventually even more biologically relevant (e.g., containing cholesterol) are currently underway.

CONCLUSIONS

The subject of equilibrium phase behavior in multicomponent lipid bilayers is a relevant and known issue. Nevertheless, experimental studies on nonequilibrium aspects of phase separation in this kind of systems are very rare. In a very recent work (Jørgensen et al., 2000), the kinetics of phase separation of equimolar lipid mixtures of $DC_{16}PC/DC_{22}PC$ was studied by Fourier-transform infrared spectroscopy and fluorescence spectroscopy (namely the variation of fluorescence intensity of a pyrene-labeled phospholipid during the course of the phase separation). In the present work, the same phenomenon was studied for a different lipid mixture ($DC_{12}PC/DC_{18}PC$ 1:1), using various photophysical techniques (variation of fluorescence intensity, fluorescence anisotropy, and FRET efficiency of suitable probes, during the equilibration process), for different final equilibrium temperatures ($T = 5$, 20, and 40°C).

While the time-scale for phase separation measured in the work of Jørgensen et al. (2000) was verified (equilibrium takes hours to be achieved after a sudden thermal quench from the one-phase region), the present study provided experimental evidence for the following aspects. 1) The time invariance of the fluorescence observables for the gel-phase probe, in contrast with the more complex, time-dependent behavior measured for the fluid phase probe, shows that whereas the gel is probably formed with properties very similar to its equilibrium properties, the fluid phase evolves from a very different nonequilibrium structure. 2) The temperature dependence study raised two additional points. One is that individual molecule diffusion (as in one-component systems) is not the only factor in the phase separation process. Gel-like molecules of the low-melting component probably act as surfactants, stabilizing the transient domain structure, and leading to slower phase separation dynamics. The other is that for lipid bilayers, as the one studied here, the driving force is related to the initial distance to equilibrium (when defined relative to the liquidus line) in a nonlinear manner, resembling spinodal decomposition. 3) The decrease of FRET efficiency between a gel phase probe and a fluid phase probe reflects most directly the dynamics of domain growth in the nanometer range. Moreover, the FRET study shows that heterogeneity is already present in the one-phase region, and after relaxation, there is either complete phase separation or the persisting domains have size larger than ~5 to 10 R_0 = 15 to 30 nm.

This work was supported by Program POCTI/FCT, Portugal, partially funded by FEDER. R. F. M. A. acknowledges a grant from PRAXIS XXI (BD 943/2000). A. F. acknowledges a FCT grant (Portugal). We thank Prof. Ole G. Mouritsen and Dr. Kent Jørgensen for helpful discussions. We are also grateful to one of the reviewers for useful comments.

REFERENCES

Almeida, P. F. F., W. L. C. Vaz, and T. E. Thompson. 1992. Lateral diffusion and percolation in two-phase, two-component lipid bilayers: topology of the solid-phase domains in-plane and across the lipid bilayer. *Biochemistry.* 31:7198–7210.

Arvinte, T., A. Cudd, and K. Hildenbrand. 1986. Fluorescence studies of the incorporation of *N*-(7-nitrobenz-2-oxa-1,3-diazol-4-yl)-labeled phosphatidylethanolamines into liposomes. *Biochim. Biophys. Acta.* 860: 215–228.

Arvinte, T., and K. Hildenbrand. 1984. *N*-NBD-L-dilauroylphosphatidylethanolamine: a new fluorescent probe to study spontaneous lipid transfer. *Biochim. Biophys. Acta.* 775:86–94.

Berberan-Santos, M. N., and M. J. E. Prieto. 1987. Energy transfer in spherical geometry: application to micelles. *J. Chem. Soc. Faraday Trans. 2.* 83:1391–1407.

Brumm, T., K. Jørgensen, O. G. Mouritsen, and T. M. Bayerl. 1996. The effect of increasing membrane curvature on the phase transition and mixing behavior of a dimyristoyl-*sn*-glycero-3-phosphatidylcholine/distearoyl-sn-glycero-3-phosphatidylcholine lipid mixture as studied by Fourier transform infrared spectroscopy and diferential scanning calorimetry. *Biophys. J.* 70:1373–1379.

Castanho, M. A. R. B., M. Prieto, and A. U. Acuña. 1996. The transverse location of *trans*-parinaric acid in lipid bilayers. *Biochim. Biophys. Acta.* 1279:164–168.

Castanho, M. A. R. B., N. C. Santos, and L. M. S. Loura. 1997. Separating the turbidity spectra of vesicles from the absorption spectra of membrane probes and other chromophores. *Eur. Biophys. J.* 26:253–259.

Chattopadhyay, A. 1990. Chemistry and biology of *N*-(7-nitrobenz-2-oxa-1,3-diazol-4-yl)-labeled lipids: fluorescent probes of biological and model membranes. *Chem. Phys. Lipids.* 53:1–15.

Chattopadhyay, A., and E. London. 1988. Spectroscopic and ionization properties of *N*-(7-nitrobenz-2-oxa-1,3-diazol-4-yl)-labeled lipids in model membranes. *Biochim. Biophys. Acta.* 938:24–34.

Chen, R., and R. L. Bowman. 1965. Fluorescence polarization: measurement with ultraviolet-polarizing filters in a spectrophotofluorometer. *Science.* 147:729–732.

Coelho, F. P., W. L. C. Vaz, and E. Melo. 1997. Phase topology and percolation in two component lipid bilayers: a Monte Carlo approach. *Biophys. J.* 72:1501–1511.

Davenport, L., R. E. Dale, R. H. Bisby, and R. B. Cundall. 1985. Transverse location of the fluorescent probe 1,6-diphenyl-1,3,5-hexatriene in model lipid bilayer membrane systems by resonance energy transfer. *Biochemistry.* 24:4097–4108.

Dolainsky, C., P. Karakatsanis, and T. M. Bayerl. 1997. Lipid domains as obstacles for lateral diffusion in suported bilayers probed at different time and length scales by two-dimensional exchange and field gradient solid state NMR. *Phys. Rev. E.* 55:4512–4521.

Edidin, M. 1998. Defining and imaging membrane domains. *Biol. Skr. Dan. Vid. Selsk.* 49:19–21.

Fung, B. K. K., and L. Stryer. 1978. Surface density determination in membranes by fluorescence energy transfer. *Biochemistry.* 17: 5241–5248.

Gliss, C., H. Clausen-Schaumann, R. Günther, S. Odenbach, O. Randl, and T. M. Bayerl. 1998. Direct detection of domains in phospholipid bilayers by grazing incidence diffraction of neutrons and atomic force microscopy. *Biophys. J.* 74:2443–2450.

Haugland, R. P. 1996. Handbook of Fluorescent Probes and Research Chemicals, 6th edition. Molecular Probes, Inc., Eugene, OR.

Hope, M. R., M. B. Bally, G. Webb, and P. R. Cullis. 1985. Production of large unilamellar vesicles by a rapid extrusion procedure: characterization of size distribution, trapped volume and ability to maintain a membrane potential. *Biochim. Biophys. Acta.* 812:55–65.

Jabłoński, A. 1960. On the notion of emission anisotropy. *Bull. Acad. Pol. Sci.* 8:259–264.

Jeppesen, C., and O. G. Mouritsen. 1993. Universality of ordering dynamics in conserved multicomponent systems. *Phys. Rev. B.* 47: 14724–14733.

Jørgensen, K., A. Klinger, and R. L. Biltonen. 2000. Nonequilibrium lipid domain growth in the gel-fluid two phase region of a DC16PC-DC22PC lipid mixture investigated by Monte-Carlo computer simulation, FT-IR and fluorescence spectroscopy. *J. Phys. Chem.* 104:11763–11773.

Jørgensen, K., and O. G. Mouritsen. 1995. Phase separation dynamics and lateral organization of two-component lipid membranes. *Biophys. J.* 95:942–954.

Korlach, J., P. Schwille, W. W. Webb, and G. W. Feigenson. 1999. Characterization of lipid bilayer phases by confocal microscopy and fluorescence correlation spectroscopy. *Proc. Natl. Acad. Sci. U.S.A.* 96:8461–8466.

Lakowicz, J. R. 1999. Principles of Fluorescence Spectroscopy, 2nd Edition. Kluwer Academic/Plenum Press, New York.

Loura, L. M. S., A. Fedorov, and M. Prieto. 1996. Resonance energy transfer in a model system of membranes: application to gel and liquid crystalline phases. *Biophys. J.* 71:1823–1836.

Loura, L. M. S., A. Fedorov, and M. Prieto. 2000a. Membrane probe distribution heterogeneity: a resonance energy transfer study. *J. Phys. Chem. B.* 104:6920–6931.

Loura, L. M. S., A. Fedorov, and M. Prieto. 2000b. Partition of membrane probes in a gel/fluid two-component lipid system: a fluorescence resonance energy transfer study. *Biochim. Biophys. Acta.* 1467:101–112.

Loura, L. M. S., A. Fedorov, and M. Prieto. 2001. Fluid-fluid membrane micro-heterogeneity: a fluorescence resonance energy transfer study. *Biophys. J.* 80:776–788.

Mabrey, S., and J. M. Sturtevant. 1976. Investigation of phase transitions of lipids and lipid mixtures by high-sensitivity differential scanning calorimetry. *Proc. Natl. Acad. Sci. U.S.A.* 73:3862–3866.

Marsh, D. 1990. Handbook of Lipid Bilayers. CRC Press, Boca Raton, FL.

Mateo, C. R., J.-C. Brochon, M. P. Lillo, and A. U. Acuña. 1993. Lipid clustering in bilayers detected by the fluorescence kinetics and anisotropy of *trans*-parinaric acid. *Biophys. J.* 65:2237–2247.

McClare, C. W. F. 1971. An accurate and convenient organic phosphorus assay. *Anal. Biochem.* 39:527–530.

Melchior, D. L. 1986. Lipid domains in fluid membranes: a quick-freeze differential scanning calorimetry study. *Science.* 234:1577–1580.

Mouritsen, O. G. 1998. Membranes display nano-scale heterogeneity: beating the randomness of the fluid lipid bilayer. *Biol. Skr. Dan. Vid. Selsk.* 49:47–53.

Mouritsen, O. G., and M. Bloom. 1984. Mattress model of lipid-protein interactions in membranes. *Biophys. J.* 46:141–153.

Mouritsen, O. G., and K. Jørgensen. 1994. Dynamical order and disorder in lipid bilayers. *Chem. Phys. Lipids.* 73:3–25.

Mouritsen, O. G., and K. Jørgensen. 1997. Small-scale lipid-membrane structure: simulation vs. experiment. *Curr. Opin. Struct. Biol.* 7:518–527.

Piknová, B., D. Marsh, and T. E. Thompson. 1996. Fluorescence-quenching study of percolation and compartmentalization in two-phase lipid bilayers. *Biophys. J.* 71:892–897.

Ruggiero, A., and B. Hudson. 1989. Critical density fluctuations in lipid bilayers detected by fluorescence lifetime heterogeneity. *Biophys. J.* 55:1111–1124.

Sackmann, E., and T. Feder. 1995. Budding, fission and domain formation in mixed lipid vesicles induced by lateral phase separation and macromolecular condensation. *Mol. Membr. Biol.* 12:21–28.

Sankaram, M. B., D. Marsh, and T. E. Thompson. 1992. Determination of fluid and gel domain sizes in two-component, two-phase lipid bilayers. *Biophys. J.* 63:340–349.

Schram, V., H.-N. Lin, and T. E. Thompson. 1996. Topology of gel-phase domains and lipid mixing properties in phase-separated two-component phosphatidylcholine bilayers. *Biophys. J.* 71:1811–1822.

Singer, S. J., and G. L. Nicolson. 1972. The fluid mosaic model of the structure of cell membranes. *Science.* 175:720–731.

Sklar, L. A., B. S. Hudson, M. Petersen, and J. Diamond. 1977a. Conjugated polyene fatty acids on fluorescent probes: spectroscopic characterization. *Biochemistry.* 16:813–818.

Sklar, L. A., B. S. Hudson, and R. D. Simoni. 1977b. Conjugated polyene fatty acids as fluorescent probes: synthetic phospholipid membrane studies. *Biochemistry.* 16:819–828.

Sklar, L. A., G. P. Miljanich, and E. A. Dratz. 1979. Phospholipid lateral phase separation and the partition of *cis*-parinaric acid and *trans*-parinaric acid among aqueous, solid lipid, and fluid lipid phases. *Biochemistry.* 18:1707–1716.

Suppan, P., and N. Ghoneim. 1997. Solvatochromism. The Royal Society of Chemistry, Cambridge, UK.

Tachyia, M. 1987. Stochastic and diffusion models of reactions in micelles and vesicles. *In* Kinetics of Nonhomogeneous Processes, G. R. Freeman, editor. Wiley-Liss, Inc., New York. 575–670.

Tomlins, P. E., and J. S. Higgins. 1989. Late stage spinodal decomposition in an oligomeric blend of polystyrene/polybutadiene: a test of the scaling law for the structure function. *J. Chem. Phys.* 90:6691–6700.

Vierl, U., L. Löbbecke, N. Nagel, and G. Cevc. 1994. Solute effects on the colloidal and phase behavior of lipid bilayer membranes: ethanol-dipalmitoylphosphatidylcholine mixtures. *Biophys. J.* 67:1067–1079.

Weber, G. 1953. Rotational Brownian motion and polarization of the fluorescence. *Adv. Protein Chem.* 8:415–459.

Wolber, P. K., and B. S. Hudson. 1981. Fluorescence lifetime and time-resolved polarization anisotropy studies of acyl chain order and dynamics in lipid bilayers. *Biochemistry.* 20:2800–2810.